

Synergistic Effect of Combining Titanosilicate and 1-Ethyl-3-Methylimidazolium Acetate in Mixed Matrix Membranes for Efficient CO₂ Separation

By M.M. López Guerrero¹, C. Casado-Coterillo², A. Irabien²

Abstract

The separation and capture of CO₂ from these sources is becoming important for greenhouse emission. The membrane-based separation process use to remove CO₂ takes advantages in energy efficient and environmentally friendly aspects and has been recognized as an important technology for CO₂ capture and gas separation. The novel mixed matrix membranes (MMMs) were fabricated by incorporating microporous titanosilicate ETS-10 and a highly CO₂ absorbent ionic liquid, [EMIM][Ac] into a Chitosan (CS) matrix to improve CO₂ separation performance, and were prepared, characterized and tested for CO₂ and N₂. The solubility values show that the CO₂ solubility increases upon addition of ETS-10 particles. The N₂ solubility in the ETS-10/[EMIM][Ac]/CS was reduced, while CO₂ solubility remained constant. FT-IR spectra revealed a good interaction between the components in the MMMs. Subtle differences in the intensity and position of all individual bands, were observed in the region between 3600 and 2700 cm⁻¹ and 1700 and 900 cm⁻¹. These indicated bonding of the components in the film, confirming the good interaction existing among the components, and that may account for the higher flexibility of the hybrid membrane materials imparted to both CS and ETS-10/CS MMMs, due to the singular interaction between CS and [EMIM][Ac].

Keywords: CO₂ solubility, CO₂ separation, microporous titanosilicate ETS-10, Chitosan, mixed matrix membranes (MMMs).

1. Introduction

Despite the significant progress in the development of new renewable energy in recent years, fossil fuels likely still occupy a dominant position in the worldwide energy source for the future (Conti 2013). Because of this situation, the separation and capture of CO₂ is becoming important for greenhouse emission and global warming, with over 30 billion tonnes of global CO₂ emissions per year in last years (McGee 2011). Economic and effective techniques for CO₂ removal are desirable and have a great interest. Conventional methods usually involve cost and complicated equipment and high energy consumption. Compare with traditional methods, the membrane based separation process has advantages in energy efficient and environmentally friendly aspects and has been recognized as an important technology for CO₂ capture and gas separation (D'Alessandro et al. 2010; Chung et al. 2007; Zhang et al. 2013; Huang et al. 2012). Membrane-based gas separation has been postulated to compete with absorption in terms of energy requirement when CO₂ content in the feed is larger than 20 % due to its low energy consumption, easy operation and low maintenance (Jiang et al. 2006). Membranes are usually classified as polymeric, inorganic, and more recently, mixed matrix membranes (MMMs). Transport through a dense-polymeric membrane usually takes place through the solution-diffusion mechanism in three steps: the selective component adsorbs in the membrane, where

¹ Department of Analytical Chemistry, Universidad de Malaga, Andalucía Tech, Malaga, Spain

² Department of Chemical and Biomolecular Engineering, Universidad de Cantabria, Santander, Spain.

diffuses through and the component desorbs from the other side, due to the low pressure kept at the permeate side.

Polymer membranes are low cost, cheaper than inorganic membranes and have good mechanical stability at high pressure. Nevertheless, polymeric membranes suffer from either low selectivity or permeability, and usually show an inverse relationship between permeability and selectivity (Zhang et al. 2013). The selectivity is regulated by the polymer molecular structure that allows preferential passing of certain gas molecules based on their sizes, normally represented by their kinetic diameters. The permeability is largely controlled by the gas solubility. The main parameter that determines the solubility is the ability of the penetrant gases to condense (Zhang et al. 2013).

Mixed matrix membranes (MMMs) are heterogeneous materials formed by the combination of an organic polymer continuous matrix and inorganic material dispersed phase, with the aim of obtaining a well-dispersed heterogeneous mixture of synergistic properties and overcoming the accepted trade-off between permeability and selectivity for gas separation membranes (Zhang et al. 2013; Robeson, 2008). Due to the chemical potential difference across membrane takes place the permeation. The permeability is usually calculated as the product of solubility (S) and diffusivity (D).

The main challenge in MMMs is the adhesion between dispersed and continuous phases. To improve adhesion, there are several strategies which have been studied, such as functionalization of the inorganic particles prior to introduction into the polymer matrix, or the incorporation of an ionic liquid in the membrane matrix (Hudiono et al. 2010; Hao et al. 2013). In a previous work, we proposed a similar approach but using a non-toxic ionic liquid, a biopolymer and a microporous zeo-type material prepared without organic surfactant (Casado-Coterillo et al. 2014b).

The components used were chitosan, a microporous titanosilicate and an ionic liquid. Chitosan (CS) is a continuous polymer, poly [$\beta(1,4)$ 2-amino-2deoxy-D-glucopyranose]. CS is a linear polysaccharide obtained by the deacetylation of chitin, which is a natural polymer, cheap, biodegradable, biocompatible, non-toxic, unique structure, interesting properties and hydrophilic. Due to their good film-forming ability, they can be used to form edible films which may provide an alternative to synthetic materials (Tharanathan 2003). High hydrophilicity makes CS prone to effective barriers against O₂, CO₂ and aromas, but their barrier properties against water are poorer which makes CS membrane effective for CO₂ separation due to the high CO₂ solubility in water (Liu et al. 2008). Furthermore, CS membranes have been well studied for CO₂ separation (Ito et al. 1997; El-Azzami and Grulke 2008; El-Azzami and Grulke 2009). Its mechanical stability has nevertheless been tried to improve by coating on a porous polysulfone support (Kai et al. 2008), organic chemical crosslinking (Xiao, Feng and Huang 2007), and physical mixing with zeolite particles (Casado-Coterillo et al. 2014).

The mechanical stability of CS has been tried to improve by coating on a porous polysulfone support (Kai et al. 2008), organic chemical crosslinking (Xiao et al. 2007), and physical mixing with zeolite particles (Casado-Coterillo et al. 2014). Facilitated transport in the solid matrix is expected to increase the stability as well, and CS, because of the weak acid-base interactions between CO₂ and water molecules and the amino groups in the chains, has potential to enhance the electrostatic interactions among permeating molecules and the functional groups in the polymer by introducing appropriate materials. Mixed matrix membranes (MMMs) have been prepared by filling the CS matrix with 5 wt. % of ETS-10 titanosilicate with synergistic transport properties in pervaporation and gas separation (Casado-Coterillo et al. 2014a, b).

The structure of the microporous titanosilicate ETS-10 is made of orthogonal TiO₆ octahedra and SiO₂ tetrahedra linked by oxygen atoms shared in the corners. Ti atoms in a six-coordinated state have two negative charges balanced by Na⁺ and K⁺ (Casado et al. 2009). The high cation exchange capacity is what makes ETS-10 very interesting in adsorption (Tiscornia et al. 2010),

catalysis, and membrane separation processes (Tiscornia et al. 2010). ETS-10 can be synthesised in different sizes including nano-scale (Casado et al. 2009), which may be homogeneously dispersed in a polymer providing this with its intrinsic characteristics. Ionic liquids (ILs) combining good and tuneable solubility properties with negligible vapour pressure and good thermal stability have recently received much attention as green solvents and CO₂ absorbents in supported liquid membrane contactors (Santos et al. 2014). The CO₂ solubility is higher when acetate is the anion and the shorter length of the cation, and 1-ethyl-3-methylimidazolium acetate, [EMIM][Ac], the room temperature ionic liquid (IL) with the highest reported CO₂ solubility (Blath et al. 2012), as well as non-reported toxicity (Alvarez-Guerra and Irabien 2011), was chosen for the proof-of-concept of this work. A good interaction with CS is expected since it has been reported as a good solvent for polysaccharides (Ding et al. 2012), because of the strong H-bonds forming with the OH groups in the polymer chain. CS and chitin have been reported to enhance the CO₂ solubility of low absorbing [bmim][Cl] because the ionic liquid is able to alter the H-bonds in the polymer chains, thus freeing amino groups that become available for CO₂ absorbing sites (Xie, Zhang and Li 2006). Novel MMMs composed of CS, [EMIM][Ac]/CS, ETS-10/CS and ETS-10/[EMIM][Ac]/CS, with the small loading of dispersed filler of 5 wt. % with respect to the continuous polymer matrix, were prepared and tested for CO₂ and N₂ permeation (Casado-Coterillo et al. 2014b). In this work, the factors affecting membrane morphology such as adhesion, interaction among components, and thermal, chemical, and mechanical resistance have been extensively explored by further FT-IR experiments and discussion complemented those of the previous work.

2. Experimental

Chitosan (coarse ground flakes and powder, Sigma-Aldrich, Madrid, Spain) with a deacetylation degree higher than 75 wt % and high viscosity in 1 wt % acetic acid/water was used. TiO₂-anatase (powder, 99.8 wt %, Aldrich, Madrid, Spain) and sodium silicate solution (27 wt % SiO₂, 8 wt % Na₂O, Merck, Barcelona, Spain) as Ti and Si source, respectively, for the ETS-10 crystal synthesis, and 1-ethyl-3-methylimidazolium acetate, [EMIM][Ac], (99%, Sigma Aldrich) were used as purchased.

2.1 Preparation of ETS-10

In a typical synthesis, 35.06 g of parent gel with molar composition 5.6 SiO₂:1 TiO₂:4.6 Na₂O:1.9 K₂O:137 H₂O were poured into a Teflon-lined autoclave and submitted to hydrothermal synthesis at 230 °C for 24 h. The autoclave was then removed from the oven and quenched under cold tap water to room temperature. The solid was washed and centrifuged at least 3 times, and dried at 100 °C overnight to recover about 2.8 g of final product. This product has a particle size of $a = b = 0.32 \pm 0.06 \mu\text{m}$ and $c = 0.41 \pm 0.22 \mu\text{m}$ and a BET surface area of $253 \pm 7 \text{ m}^2/\text{g}$.

2.2 Preparation of membranes.

The preparation of the pure CS and CS-based MMMs has been reported elsewhere (Casado-Coterillo et al. 2014). In a typical synthesis, first, CS 2 wt. % solutions were first dissolved in 2 wt. % acetic acid (glacial, Panreac) aqueous solutions under stirring at 80 °C for 24 h at reflux conditions. The CS solution obtained was filtered to remove insoluble impurities and degassed in an ultrasonic bath before 10 mL on a polystyrene Petri dish and evaporating at room temperature for 2–3 days. CS membranes were then removed from the Petri dish. A 15.55 cm² membrane was cut from the film for gas permeation and neutralized in 1 M NaOH and rinsed with abundant distilled water and dried at 4 °C before CO₂ and N₂ permeation experiments in

order to ion-exchange the NH_3^+ functional groups of the polymer matrix. ETS-10 particles were first dispersed in distilled water (proportion 1:100 wt/wt) in an ultrasound bath for 10 min at room temperature. Then, CS solution (10 mL) was added and treated in ultrasound bath for 15 min until a homogenous white dispersion was obtained and cast as described above. IL/CS membranes were prepared with a nominal 5 wt. % IL loading with respect to CS. In a typical synthesis: 0.042 g of IL (97 wt. %, Sigma-Aldrich, Madrid, Spain) were added to the 10 mL CS solution and stirred overnight before casting in a similar manner as the pure CS membranes. For the three-component ETS-10/[EMIM][Ac]/CS MMMs, the preparation method was similar to that employed for ETS-10/CS MMMs, using the [EMIM][Ac]/CS mixture as continuous phase.

2.3 Equipment

IR Spectra were recorded on a Perkin Elmer Spectrum 100 FTIR spectrometer (Perkin Elmer, Concord, Canada) with a resolution of 4 cm^{-1} and 32 accumulations. Solid samples were measured by using potassium bromide pellets. The solid samples were dried at $100\text{ }^\circ\text{C}$ for at least 2 h and grinded for 5 min, the concentrations for the samples were 10 wt. % approximately. Per sample sample/KBr mixture (approx. 10/100 wt/wt and 100 mg in total) were made. Also one KBr was made as a reference.

The liquid sample was measured using optical transmission cell, having windows compatible with infrared wavelengths. All cells used had planar windows and the liquid samples were measured dripping several drops of the sample between two thin pieces of glass and sandwiching it. In both cases, the absorbance values were determined between 4000 and 450 cm^{-1} .

The mechanical resistance of the membranes was measured by the tensile strength and the elongation at break of 5–10 of 5 mm wide samples of the membrane materials in a Universal Testing Machine (Zwick/Roell, Ulm, Germany) with a head load up to 2.5 kN and 5 mm/min.

3. Results and Discussion

3.1 FT-IR spectra

In order to characterize the initial materials, a spectrum of pure chitosan was recorded (Fig.1a). The main bands appearing in the spectrum of chitosan (CS) powder is due to stretching vibrations of OH groups in the range from 3750 cm^{-1} to 3000 cm^{-1} and C–H bond in $-\text{CH}_2$ (2930 cm^{-1}) and $-\text{CH}_3$ (2875 cm^{-1}) groups, respectively. Bending vibrations of methylene and methyl groups were also visible at 1380 cm^{-1} and 1460 cm^{-1} , respectively (Mano et al., 2003). The range of 1680 – 1480 cm^{-1} was related to the vibrations of carbonyl bonds (C=O) of amide group CONHR (secondary amide, 1660 cm^{-1}) and to the vibrations of amine group NH_2 , 1580 cm^{-1} (Ruel-Gariépy and Leroux, 2006). The spectra in the range from 1160 cm^{-1} to 1000 cm^{-1} have been analysed by many authors who attribute vibrations appearing in this range to CO group (Duarte et al. 2002; Xu et al. 2005). The band located near 1150 cm^{-1} is related to asymmetric vibrations of CO in oxygen bridge. Resulting from deacetylation of chitosan. The bands near 1080 – 1025 cm^{-1} are attributed to CO of the ring COH, COC and CH_2OH (Duarte et al. 2002; Shigemasa et al. 1996; Nunthanid et al. 2001).

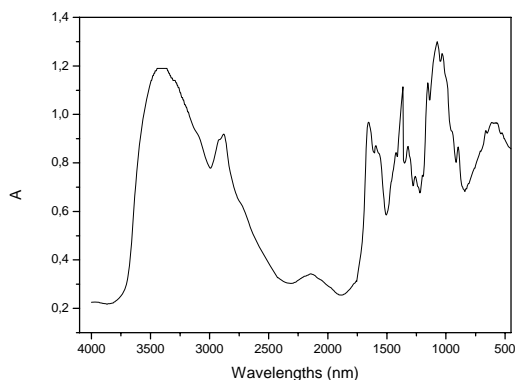


Figure 1a. Chitosan FT-IR spectrum.

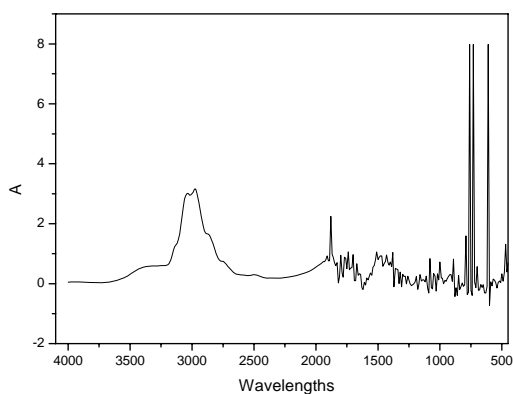


Figure 1b. EMIM Ac FT-IR spectrum

On the other hand, the [EMIM]-Ac ionic liquid shows a characteristic absorption pattern between 1700 and 600 cm^{-1} , Fig. 1b. In the fingerprint region, that is, in the spectral range below 1500 cm^{-1} , numerous peaks overlapping with each other are observed. Nevertheless, several characteristic features can be assigned to their vibrational modes. The main contributions found in the spectral range between 500 and 1000 cm^{-1} can be attributed to the [EMIM] cation. An in-plane symmetric bending mode of the ring, with contribution from a $\text{CH}_3(\text{N})\text{CN}$ stretching mode, is found at 600 cm^{-1} . Asymmetric bending of the ring HCCH group shows up at 756 cm^{-1} , and a ring bending vibration from the $\text{NC}(\text{H})\text{N}$ group, with contribution from the CCH bending, is found at 845 cm^{-1} . CC stretching is observed at 958 cm^{-1} . Substantial contributions from the acetate anion are found in the spectral range between 1000 and 2000 cm^{-1} (along with further lines from the [EMIM] cation). A ring in-plane asymmetric stretching, with contributions from the $(\text{N})\text{CH}_2$, $\text{CH}_3(\text{N})\text{CN}$, and CC stretching, results in a strong peak at 1169 cm^{-1} . The $\text{C}-\text{CH}_3$ stretching vibration from acetate is found at 1254 cm^{-1} , whereas the bending mode of CH_3 is present at 1425 cm^{-1} . In between (at 1389 cm^{-1}), another strong line attributed to [EMIM] is observed, where a ring in-plane asymmetric stretching, a $\text{CH}_2(\text{N})$ bending, a CC stretching, a $\text{CH}_2(\text{N})$ stretching, and a $\text{CH}_3(\text{N})\text{CN}$ stretching overlap. The $\text{C}=\text{O}$ stretching band is found at 1566 cm^{-1} (this signal is normally located at around

1700 cm^{-1} in non-ionic carbonyl compounds). This frequency shift can be explained by both a delocalization of the electrons in the ionic acetate compound and substantial intermolecular interactions with the [EMIM] cation, which influence the vibrational structure.

A number of comparatively weak overlapping CH stretching modes is observed in the range 2900–3200 cm^{-1} , whereas a broad band corresponding to the intermolecular O-H vibrations caused by hydrogen bonds is present between 3200 and 3700 cm^{-1} (Kiefer et al 2008).

It is well-known that in the region of 3800 – 3000 cm^{-1} the water vibration is present. It is important to note that dry [EMIM][Ac] does not have absorptions in this region. This is very interesting, since we have observed that the introduction of the ionic liquid in the chitosan matrix greatly reduces the water swelling of the chitosan matrix, thus improving the flexibility of the films. These might help correlating FTIR to the data on Table 1.

The molecules produce a broad band in the region around 3450 cm^{-1} . The strengthening of O-H stretching vibration band is due to the interactions between [EMIM] [Ac] and water. The water would easily be absorbed due to forming strong H-bonds with the anion of [EMIM] [Ac].

In this spectrum the vibrational frequencies of 1-ethyl-3-methylimidazolium cation, acetate anion, and C1 and C2 conformers of their ion pair are shown. The IR bands at 1005, 1120, 1170 and 1647 cm^{-1} agree with the vibrational structure of the C1 conformer. This suggests that the C1 conformer is the major contributor to the vibrational structures observed in the experimental spectra. C2-H13 stretching frequency by ~ 1197 cm^{-1} in the C1 conformer with respect to the free cation value 3203 cm^{-1} . This dramatic shift is attributed to the strong C-H \cdots O interaction between the cation and anion considered (Nilesh et al. 2009).

The 1647 cm^{-1} band observed in the IR spectrum is assigned to the O9-C10 local stretching mode combined with N3-C4-H14 rocking vibrations (Nilesh et al. 2009).

Turning to ethyl and methyl groups of the cation, bending vibrations are generally in good agreement with measurements, for instance, the bands appearing at frequencies 1449 and 1454 cm^{-1} are assigned to H19-C7-H20 twisting vibrations. Likewise, bands at 1388 and 1393 cm^{-1} are attributed to the intense mode arising from H21-C8-H22 rocking vibrations. While the assignment is very reasonable, we nevertheless point out that the IR peak at 1388 cm^{-1} could be assigned instead to the C10-C12 stretching vibrations of the acetate anion in the ion pair (Dumal et al. 2009).

When two or more substances are mixed, physical blends versus chemical interactions are reflected by changes in characteristic spectra peaks. Furthermore, the increased flexibility imparted to the MMMs by the introduction of the IL was attributed to the singular interaction between CS and IL, and due to this fact, the FT-IR spectra of the membranes were measured and studied (Figure 2).

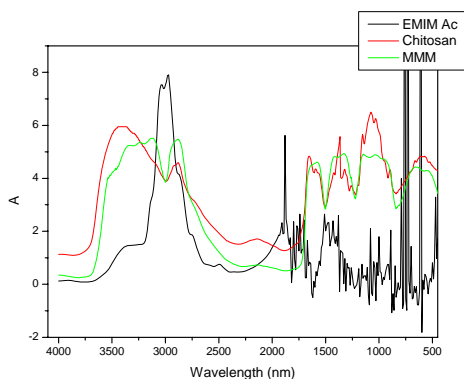


Figure 2. FT-IR of MMMs, CS and EMIM Ac.

Subtle differences in the intensity and position of all individual bands, observed both in the region between 3600 and 2700 cm^{-1} and between 1700 and 900 cm^{-1} , clearly indicated bonding of the components of the film. In the first region, between 3600 and 2700 cm^{-1} , as a result of the formation of the three-component film, the absorption bands at 3280 and 2940 cm^{-1} of MMM decreased in intensity and moved by 5 and 10 cm^{-1} , respectively, to lower wave numbers. The CS and 3-component ETS-10/IL/CS membranes demonstrated a broad band in the range 3600–2700 cm^{-1} , attributed to NH and OH vibrations, whereas the broad band at around 2940 cm^{-1} in CS is shifted to lower wave numbers due to film formation.

The modified band around 2940 cm^{-1} might reflect these conformational changes of the polymer chains.

In the second region, between 1700 and 900 cm^{-1} , the amide I, amide II and amide III bands decreased in intensity due to the formation of the three-component film. That trend followed former findings revealed by Taravel and Domard (1995). Moreover, a band at 1377 cm^{-1} of chitosan, in the spectrum of the MMM could be recognized as a shoulder of the peak at 1410 cm^{-1} . The shift of the latter by 10 cm^{-1} towards higher wave numbers compared with its location in the spectrum of the film pointed at participation of the $-\text{COO}^-$. This confirms the good interaction existing among the components involved on MMM preparation, and that may account for the higher flexibility of the hybrid membrane materials imparted to both CS and ETS-10/CS MMMs, as explained above regarding mechanical properties of the membranes in Table 1.

3.2 Other membrane properties.

Other properties of the MMMs were evaluated in a previous work and correlated the observations of FTIR experiments discussed above, regarding the synergic effect of the use of ETS-10 particles and [EMIM][Ac] ionic liquid as fillers to the CS matrix. The crystallinity, χ , of the CS-based membrane samples was also calculated from the FTIR spectra, using the ratio of the absorbance at 1423 and 890 cm^{-1} , respectively. The crystallinity increased monotonously upon addition of [EMIM][Ac], ETS-10 and both to the CS polymer matrix, as reported for other MMMs prepared from semi-crystalline polymers (Shen and Luca, 2012), where this phenomenon was attributed to the role of inorganic fillers as nucleating agents. The crystallinity is important in membrane analysis since only the amorphous part of the polymer is contributing to the gas separation.

The tensile strength diminishes upon addition of [EMIM][Ac] and ETS-10 particles. This was attributed to plasticization of the polymer matrix reflected by the large increase on the value of the elongation at break, for the [EMIM][Ac]/CS with respect to CS membranes. The introduction of [bmim][CF₃SO₃] IL in semi crystalline Pebax polymers (Bernardo et al. 2012) caused a decrease in the elongation at break that has not been observed here. On the other hand, the elongation at break of the CS-based membranes decreases upon addition of ETS-10 particles. This is due to the rigidification of the organic polymer (Xu et al. 2011) by the addition of inorganic fillers.

Table 1. MMMs properties (Casado-Coterillo et al. 2014)

Membrane material composition	Thickness (μm)	Tensile strength (MPa)	Elongation at break (%)	$\chi(-)$	$S(\text{CO}_2)$ $\text{cm}^3(\text{STP})/\text{cm}^3$ Hg	$S(\text{N}_2)$ $\text{cm}^3(\text{STP})/\text{cm}^3$ Hg
CS	121.9 \pm 3.9	31.6 \pm 7.4	18.5 \pm 7.4	0.14	0.08	0.005
[EMIM][Ac]/CS	128.0 \pm 3.6	16.1 \pm 11.0	40.4 \pm 11.0	0.18	0.51	0.026
ETS-10/CS	130.0 \pm 4.5	24.3 \pm 4.9	14.4 \pm 9.4	0.28	0.08	0.003
ETS-10/[EMIM][Ac]/CS	168.0 \pm 5.0	19.9 \pm 5.0	36.2 \pm 3.0	0.34	0.07	0.002

The solubility values were calculated from the thermogravimetric sorption experiments. As it was said previously, CS shows a high hydrophilicity that makes CS prone to enhanced CO₂: N₂

perm-selectivity, ETS-10 shows a high exchange capacity, which is very interesting in adsorption, and [EMIM][Ac] shows good solubility properties. The combination of these three components increases the solubility of CO₂ due to the H-bonds in the polymer chains, thus freeing amino groups that become available for CO₂ absorbing sites (Xie et al. 2006). The solubility increases upon addition of ETS-10, due to its adsorption affinity toward CO₂. On the other hand, the N₂ solubility decreases in ETS-10/CS MMMs, due to the molecular sieve effect of the nanoporous titanosilicate. The N₂ solubility in MMMs was decreased, because of the incorporation of CO₂-soluble IL, while CO₂ solubility remained constant, compared with the two-component ETS-10/CS MMM (Casado-Coterillo et al. 2014).

4. Conclusion

FT-IR spectra revealed a good interaction between the components in the MMMs. The FT-IR are proven to be the efficient methods for the characterization of the interaction between [EMIM][Ac], ETS-10 and CS. The shift of the vibrational frequency has been used to correlate the relative strength of H-bond. The CO₂ solubility increased upon addition of both the [EMIM][Ac] and ETS-10 adsorbent, the mechanical strength was enhanced and the selectivity was six times higher than pure CS membrane, thus leading to a synergistic effect on the membrane properties as a result of the good interaction between the components.

Acknowledgements

Financial support from the Spanish Ministry of Economy and Competitiveness (MINECO) under project CTQ2012-31229 is gratefully acknowledged.

References

- Alvarez-Guerra, M.; Irabien, A. (2011) Design of ionic liquids: An ecotoxicity (*Vibrio fischeri*) discrimination approach. *Green Chem.*, 13: 1507–1516.
- Bernardo, P.; Jansen, J.C.; Bazzarelli, F.; Tasselli, F.; Fuoco, 2012, A. Gas transport properties of Pebax (R) /room temperature ionic liquid gel membranes. *Sep. Purif. Technol.* 97: 73–82.
- Blaht, J.; Deubler, N.; Hirth, T.; Schiestel, T. (2012) Chemisorption of carbon dioxide in imidazolium based ionic liquids with carboxylic anions. *Chem. Eng. J.*, 181–182, 152–158.
- Casado, C.; Amghouz, Z.; García, J.R.; Boulahya, K.; González-Calbet, J.M.; Téllez, C.; Coronas, J. (2009) Synthesis and characterization of microporous titanosilicate ETS-10 obtained with different Ti sources. *Mater. Res. Bull.* 44: 1225–1231.
- Casado-Coterillo, C.; Andrés, F.; Téllez, C.; Coronas, J.; Irabien, A. (2014) Synthesis and characterization of ETS-10/chitosan nanocomposite materials for pervaporation. *Sep. Sci. Technol.* 49: 1903-1909.
- Casado-Coterillo, C.; López-Guerrero, M. d. M. and Irabien A. (2014) Synthesis and characterisation of ETS-10/Acetate-based ionic liquid/chitosan mixed matrix membranes for CO₂/N₂ separation. *Membranes*, 2014, 4 (2): 287-301.
- Chung, T.S., Jiang, L.Y., Li, Y., Kulprathipanja, S., (2007) Mixed matrix membranes (MMMs) comprising organic polymers with dispersed inorganic fillers for gas separation, *Prog. Polym. Sci.* 32: 483–507.
- D'Alessandro, D.M., Smit, B., Long, J.R., (2010) Carbon dioxide capture: prospects for new materials, *Angew. Chem. Int. Ed.* 49: 6058–6082.
- Ding, Z.-D.; Chi, Z.; Gu, W.-X.; Gu, S.-M.; Liu, J.-H.; Wang, H.J. (2012) Theoretical and experimental investigation on dissolution and regeneration of cellulose in ionic liquid. *Carbohydr. Polym.* 89: 7–16.
- Duarte, M.L., Ferreira, M.C., Marvao, M.R., Roh, J. (2002) [An optimised method to determine the degree of acetylation of chitin and chitosan by FTIR spectroscopy](#). *Int. J. Biol. Macromol.* 31: 1-8.
- Dumal, N. R., Kim, H. J., Kiefer, J. 2009 Molecular interactions in 1 ethyl 3 methylimidazolium acetate ion pair: a density functional study. *J. Phys Chem. A.* 113: 10397-10404.
- El-Azzami, L.A.; Grulke, E.A. (2008) Carbon dioxide separation from hydrogen and nitrogen by fixed facilitated transport in swollen chitosan membranes. *J. Membr. Sci.* 323: 225–234.

- El-Azzami, L.A.; Grulke, E.A. (2009) Parametric study of CO fixed carrier facilitated transport through swollen chitosan membranes. *Ind. Eng. Chem. Res.* 48, 894–902.
- Freeman, B.D. (1999) Basis of permeability/selectivity trade-off relations in polymeric gas separation membranes. *Macromol*32, 375–380.
- Hao, L.; Li, P.; Yang, T.; Chung, T.S. (2013) Room temperature ionic liquid/ZIF-8 mixed-matrix membranes for natural gas sweetening and post-combustion CO₂ capture. *J. Membr. Sci.* 436: 221–231.
- Huang, A., Wang, N., Kong, C., Caro, J., (2012) Organosilica-functionalized zeolitic imidazolate framework ZIF-90 membrane with high gas-separation performance, *Angew. Chem. Int. Ed.* 51: 10551–10555.
- Hudiono, Y.C.; Carlisle, T.K.; Bara, J.E.; Zhang, Y.; Gin, D.L.; Noble, R.D. (2010). A three-component mixed-matrix membrane with enhanced CO₂ separation properties based on zeolites and ionic liquid materials. *J. Membr. Sci.* 350: 117–123.
- Conti J., *International energy Outlook, DOE/EIA-0484, U.S. Independent Statistics and Analysis, U.S. Energy Information Administration, Washintong DC, 2013. On the web; www.eia.gov/ieo/, last consulted on 30/03/2015.*
- Ito, A.; Sato, M.; Anma, T. (1997) Permeability of CO₂ through chitosan membrane swollen by water vapor in feed gas. *Angew. Makromol. Chem.* 248: 85–94. 14.
- Jiang, L.Y., Chung, T.S., Kulprathipanja, S. (2006) Fabrication of mixed matrix hollow fibers with intimate polymer-zeolite interface for gas separation. *AIChE J.* 52: 2898–2908.
- Kai, T.; Kouketsu, T.; Duan, S.; Kazama, S.; Yamada, K. (2008) Development of commercial-sized dendrimer composite membrane modules for CO₂ removal from flue gas. *Sep. Purif. Technol.* 63: 524–530. 17.
- Kiefer, J., Obert, K., Bösmann, A., Seeger, T., Wasserscheid, P., Leiertz, A. (2008) Quantitative analysis of alpha-D-glucose in an ionic liquid by using infrared spectroscopy. *Chem Phys Chem.* 9: 1317–1322.
- Liu, L.; Chakma, A.; Feng, X. (2008) Gas permeation through water-swollen hydrogel membranes. *J. Membr. Sci.*, 310: 66–75.
- Mano, J.F., Koniarova, D., Reis, R.L., (2003) Thermal properties of thermoplastic starch/synthetic polymer blends with potential biomedical applicability. *medicine. Mater. Sci. Mater. Med.* 14: 127–136.
- Ruel-Gariépy, E. and Leroux J.C. Chitosan: a natural polycation with multiple applications. In: Marcessault, R.H., Ravenelle, F., Zhu, XX. *Polysaccharides for drug delivery and pharmaceutical applications*, American Chemical Society, Washington 2006: 243-259.
- McGee, M. CO₂ now, <http://CO2now.org/Current-CO2/CO2-now/global-carbon-emissions.html>, 2011, last consulted on 29/03/2015.
- Nilesh, R. D., Hyung, J.K., Johannes, K. (2009), Molecular Interactions in 1-Ethyl-3-methylimidazolium Acetate Ion Pairs: A density Functional Study, *J Phys. Chem.* 113, 10397-10404.
- Nunthanid, J., Puttipatkahachorn, S, Yamamoto, K., Peck, G.E. (2001), Physical properties and molecular behavior of chitosan films, *Drug Dev. Ind. Pharm.* 27: 143-157.
- Robeson, L.M. (2008) The upper bound revisited. *J. Membr. Sci.* 320, 390–400.
- Santos, E.; Albo, J.; Irabien, A. (2014) Acetate based supported ionic liquid membranes (SILMs) for CO₂ separation: Influence of the temperature. *J. Membr. Sci.*, 452: 277–283.
- Shen, Y., Luca. A.c., (2012) Preparation and characterization of mixed matrix membranes based on PVDF and three inorganic fillers (fumed nonporous silica, zeolite 4A and mesoporous MCM-41) for gas separation. *Chem. Eneg. J.*,122: 427-435.
- Shigemasa, Y., Matsuura, H., Sasmoto, H., Sashiwa, H., (1996) Evaluation of Different Absorbance Ratios from Infrared Spectroscopy for Analyzing the Degree of Deacetylation in Chitin. *Int. J. Biol. Macromol.* 18: 237-242.
- Taravel M.N., Domard, A. (1995) Collagen and its interaction with chitosan. *Biomaterials* 18: 865-871.
- Tharanathan., R. N. (2003) [Biodegradable films and composite coatings: past, present and future](#). *Trend. Food Sci. Technol.* 14: 71-78.
- Tiscornia, I.; Irusta, S.; Prádanos, P.; Téllez, C.; Coronas, J.; Santamaría, J. (2007) Preparation and characterization of titanosilicate Ag-ETS-10 for propylene and propane adsorption. *J. Phys. Chem. C.* 111: 4702–4709.
- Tiscornia, I.; Kumakiri, I.; Bredesen, R.; Téllez, C.; Coronas, J. (2010) Microporous titanosilicate ETS-10 membrane for high pressure CO₂ separation. *Sep. Purif. Technol.* 73: 8–12.

- Xiao, S.; Feng, X.; Huang, R.Y.M. (2007) Trimesoyl chloride crosslinked chitosan membranes for CO₂/N₂ separation and pervaporation dehydration of isopropanol. *J. Membr. Sci.* 306: 36–46.
- Xie, H.; Zhang, S.; Li, S. (2006) Chitin and chitosan dissolved in ionic liquids as reversible sorbents of CO₂. *Green Chem.*, 8: 630–633.
- Xu, D.; Loo, L.S.; Wang, K. Characterization and diffusion behaviour of chitosan-POSS composite membranes. *J. Appl. Polym. Sci.* 2011, 122, 427–435.
- Xu, Y., Kim, K., Hanna, M., Nag, D., (2005) Chitosan-starch composite films preparation and characterization. *Ind. Crop. Prod.* 21: 185-192
- Zhang, C., Xiao, Y., Liu, D., Yang, Q., Zhong, C., (2013) A hybrid zeolitic imidazolate framework membrane by mixed-linker synthesis for efficient CO₂ capture, *Chem. Commun.* 49: 600–602.
- Zhang, Y., Sunarso, J., Liu, S., Wang, R. (2013) Current status and development of membranes for CO₂/CH₄ separation: a review, *Int. J. Greenh. Gas Cont.* 12: 84–107.